A Compact Photonics-Based Single Sideband Mixer Without Using High-Frequency Electrical Components
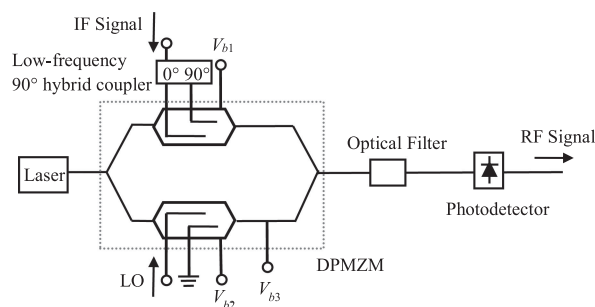
Chongjia Huang
Erwin H. W. Chan, *Senior Member, IEEE*
Chirappanath B. Albert

A Compact Photonics-Based Single Sideband Mixer Without Using High-Frequency Electrical Components

Chongjia Huang, Erwin H. W. Chan ⓘ **,** *Senior Member, IEEE,*
and Chirappanath B. Albert

College of Engineering, IT and Environment, Charles Darwin University, Darwin, NT 0909,
Australia

Abstract: A new microwave photonic frequency up converter is presented. It is capable
to generate an up converted upper or lower sideband RF signal with the other sideband
and the LO being suppressed. Compared to the reported photonics-based single sideband
(SSB) frequency up converters, the proposed structure is simple and does not require
high-frequency electrical components. The upper or lower sideband can be selected by
controlling a modulator bias voltage. The new photonics-based SSB mixer is experimentally
verified. Around 30 dB suppression in the undesired frequency components adjacent to the
up converted RF signal is demonstrated for different input LO and IF signal frequencies
when the SSB mixer is operated in either upper or lower sideband mode.

Index Terms: Optical fibre communication, frequency conversion, microwave mixer, optical
signal processing, optical modulators.

1. Introduction

Transmitting radio frequency (RF) signals through optical fibres, which is referred to as radio-over-fibre (RoF), is widely used in today's communication. Its applications include transmission of mobile radio signals, cable television signals, radar signals, and signals for satellite communications. One of the signal processing functions in RoF systems is microwave frequency conversion [1]. A frequency up converter converts a low-frequency intermediate frequency (IF) signal into a high-frequency RF signal by mixing the IF signal with a high-frequency local oscillator (LO). Realising microwave frequency up conversion in the optical domain has the advantages of wide bandwidth, immunity to electromagnetic interference, high isolation, and compatible with fibre-based transmission systems. Hence various microwave photonic frequency up conversion techniques have been developed. They are based on using either electro-optic mixing in a Mach Zehnder modulator (MZM) [2] and in a phase modulator together with dispersion effect in an optical fibre [3], cross absorption modulation in an electroabsorption modulator (EAM) [4], cross phase modulation in semiconductor optical amplifiers [5] or stimulated Brillouin scattering (SBS) in a single mode fibre [6]. All these techniques require a subsequent filtering operation to remove the LO and the undesired sideband present at the mixer output. For example, considering a 10 Mb/s QPSK data at 100 MHz IF is up converted to the 60 GHz band in a RoF system [7]. The output of a frequency up converter implemented
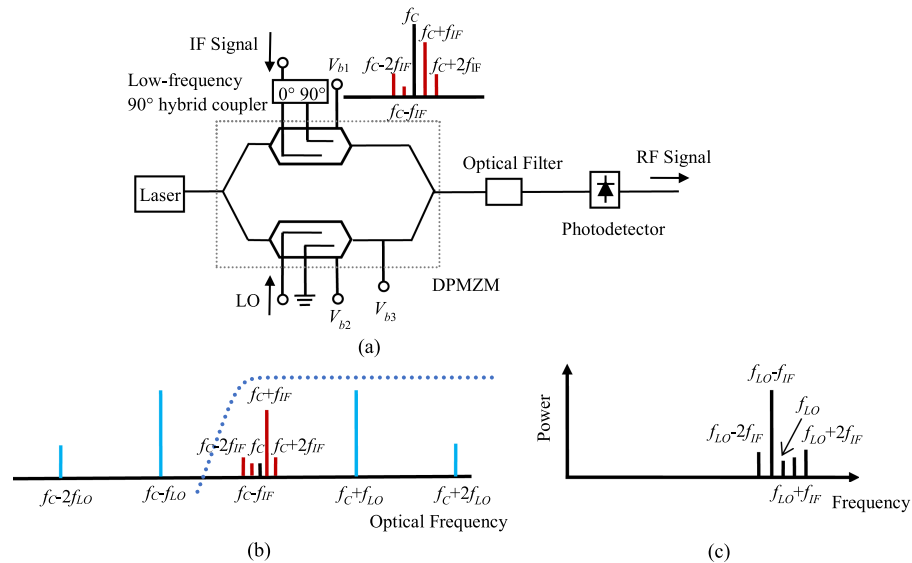
Fig. 1. (a). Structure of the DPMZM based microwave photonic SSB mixer. (b). Optical spectrum at the DPMZM output and the optical filter amplitude response (dotted line). (c). SSB mixer output electrical spectrum showing the up converted RF signal at $f_{LO} - f_{IF}$ together with the undesired frequency components. f_c: optical carrier frequency, f_{IF}: IF signal frequency, f_{LO}: LO frequency.

using the techniques discussed above consists of a lower sideband (LSB) at 59.9 GHz, a LO at 60 GHz and an upper sideband (USB) at 60.1 GHz. A high-resolution filter is required to remove the LO and the undesired sideband. Multiple filters with different centre frequencies are needed for up converting IF signals into multiple different-frequency RF signals [8] and the centre frequencies of the filters need to be tuned as the output RF signal frequencies change. This largely increases the system complexity.

A single sideband (SSB) mixer, which generates only one sideband with the LO being suppressed, can be used to overcome the problem. Recently there are few reports on microwave photonic SSB mixers. They rely on using one or more electrical 90° hybrid coupler to generate two quadrature-phase high-frequency LO and IF signals into a dual-parallel Mach Zehnder modulator (DPMZM) [9] or into a dual-polarisation dual-parallel Mach Zehnder modulator (DP-DPMZM) [10], or to combine the high-frequency RF signals after two photodetectors [11], [12]. The 90° hybrid couplers used in the reported SSB mixers [9]–[12] need to operate at high frequencies, which not only limits the system bandwidth but also has large frequency-dependent amplitude and phase imbalance. This requires adjusting system parameters as the LO frequency changes to maintain a high suppression ratio in the LO and the undesired sideband. A microwave photonic SSB mixer without using a high-frequency electrical 90° hybrid coupler has been reported [13]. However, it requires a high-frequency electrical splitter to split an LO into two before applying them into a DP-DPMZM. A high-frequency electrical splitter also has a frequency-dependent amplitude and phase imbalance characteristic and the DP-DPMZM used to implement the SSB mixer needs six DC bias voltages. In this paper, a simple photonics-based SSB mixer is proposed and experimentally demonstrated. It is based on a single-laser and single-photodetector structure with a DPMZM for frequency up conversion. It does not require high-frequency electrical components. Experimental results demonstrate around 30 dB suppression in the undesired frequency components adjacent to the up converted RF signal.

2. Operation Principle and Analysis

The structure of the proposed SSB mixer is shown in Fig. 1(a). It consists of a laser, a DPMZM, an optical filter and a photodetector. The DPMZM has two sub dual-drive MZMs (DDMZMs) connected in parallel in a main MZM. Each sub-DDMZM has two RF ports for microwave signal modulation.

The phase difference between the two arms of the two sub-DDMZMs and the two arms of the main MZM are controlled by three DC bias voltages (V_{b1}, V_{b2} and V_{b3}). The top DDMZM is biased at the quadrature point and is driven by two low-frequency quadrature-phase IF signals. The electric field at the output of the top DDMZM is given by

$$E_{DDMZM1}(t) = \frac{E_{in}\sqrt{t_{ff}}}{2\sqrt{2}}\left[\cos\left(2\pi f_c t + \beta_{IF}\sin\left(2\pi f_{IF}t + \frac{\pi}{2}\right)\right) + \cos\left(2\pi f_c t + \beta_{IF}\sin\left(2\pi f_{IF}t\right) + \frac{\pi}{2}\right)\right] \tag{1}$$

where E_{in} is the electric field amplitude of the continuous wave (CW) light into the DPMZM, t_{ff} is the insertion loss of the DDMZM, $\beta_{IF} = \pi V_{IF}/V_\pi$ is the IF signal modulation index, V_{IF} is the voltage of the IF signal into each electrode of the top DDMZM, V_π is the DDMZM switching voltage, and f_c and f_{IF} are the frequency of the optical carrier and the IF signal respectively. Note that a DDMZM can be modelled as two optical phase modulators connected in parallel. The two cosine terms inside the square brackets in (1) are the electric fields of the two phase modulated optical signals. Considering all frequency components up to and including the second order sidebands, (1) can be written as

$$E_{DDMZM1}(t) = \frac{E_{in}\sqrt{t_{ff}}}{2\sqrt{2}}\left[\begin{array}{c}\sqrt{2}J_0(\beta_{IF})\cos\left(2\pi f_c t + \frac{\pi}{4}\right) - 2J_1(\beta_{IF})\sin\left(2\pi\left(f_c + f_{IF}\right)t\right) \\ -\sqrt{2}J_2(\beta_{IF})\cos\left(2\pi\left(f_c + 2f_{IF}\right)t - \frac{\pi}{4}\right) - \sqrt{2}J_2(\beta_{IF})\cos\left(2\pi\left(f_c - 2f_{IF}\right)t - \frac{\pi}{4}\right)\end{array}\right] \tag{2}$$

where $J_n(x)$ is the Bessel function of nth order of the first kind. Equation (2) shows the first order lower IF sideband at $f_c - f_{IF}$ is eliminated. The first order upper IF sideband has a phase difference of $\pm\pi/4$ compared to the optical carrier and the two second order IF sidebands. The $\pm\pi/4$ optical phase difference is originated from the two 90° phase difference IF signals into a quadrature-biased DDMZM. A high-frequency LO is applied to one of the bottom DDMZM RF ports, which is also biased at the quadrature point. The electric field at the output of the bottom DDMZM is given by

$$E_{DDMZM2}(t) = \frac{E_{in}\sqrt{t_{ff}}}{2\sqrt{2}}\left[\cos\left(2\pi f_c t + \beta_{LO}\sin\left(2\pi f_{LO}t\right)\right) + \cos\left(2\pi f_c t + \frac{\pi}{2}\right)\right] \tag{3}$$

where $\beta_{LO} = \pi V_{LO}/V_\pi$ is the LO modulation index, V_{LO} is the voltage of the LO into the bottom DDMZM and f_{LO} is the frequency of the LO. Considering all frequency components up to and including the second order sidebands, (3) can be written as

$$E_{DDMZM2}(t) = \frac{E_{in}\sqrt{t_{ff}}}{2\sqrt{2}}\left[\begin{array}{c}\sqrt{J_0^2(\beta_{LO}) + 1}\cos\left(2\pi f_c t + \tan^{-1}\left(\frac{1}{J_0(\beta_{LO})}\right)\right) \\ +J_1(\beta_{LO})\cos\left(2\pi\left(f_c + f_{LO}\right)t\right) - J_1(\beta_{LO})\cos\left(2\pi\left(f_c - f_{LO}\right)t\right) \\ +J_2(\beta_{LO})\cos\left(2\pi\left(f_c + 2f_{LO}\right)t\right) + J_2(\beta_{LO})\cos\left(2\pi\left(f_c - 2f_{LO}\right)t\right)\end{array}\right] \tag{4}$$

The LO power is designed so that the optical carrier in the bottom arm of the main MZM has the same amplitude as that in the top arm. The main MZM is biased at the null point. This introduces a 180° phase shift to the optical signal travelled in the bottom arm of the main MZM. Hence the optical carriers in the two arms of the main MZM cancel out each other at the output of the DPMZM. The output of the DPMZM, which has an optical spectrum as shown in Fig. 1(b), consists of three main frequency components. They are the upper IF sideband at $f_c + f_{IF}$, and the two LO sidebands at $f_c \pm f_{LO}$. Since the mixer is designed to be used for frequency up conversion, the LO sidebands are located far away from the optical carrier. An optical filter is connected to the DPMZM output to filter out the lower LO sidebands. An example of an optical filter that can be used in the SSB mixer shown in Fig. 1(a) is a commercial low-cost thin film optical filter. It has an amplitude response as shown by the dotted line in Fig. 1(b) that can be described by a Butterworth filter transfer function [14], which is given by

$$H(f) = \frac{1}{\sqrt{1 + \left(\frac{f - f_{centre}}{f_{BW}/2}\right)^{2n}}} \tag{5}$$

where f_{centre} is the optical filter centre frequency, f_{BW} is the optical filter 3-dB bandwidth and n is the order of the Butterworth filter. The filter centre frequency and bandwidth can be designed to obtain a large suppression in the lower LO sideband. The electric field at the output of the optical filter can be written as

$$
E_o(t) = \frac{E_{in}\sqrt{t_{ff}}}{4}
\begin{bmatrix}
\sqrt{2}J_0\left(\beta_{IF}\right)\cos\left(2\pi f_c t + \frac{\pi}{4}\right) - \sqrt{J_0^2\left(\beta_{LO}\right)+1}\cos\left(2\pi f_c t + \tan^{-1}\left(\frac{1}{J_0(\beta_{LO})}\right)\right) \\
-2J_1\left(\beta_{IF}\right)\sin\left(2\pi\left(f_c + f_{IF}\right)t\right) - \sqrt{2}J_2\left(\beta_{IF}\right)\cos\left(2\pi\left(f_c + 2f_{IF}\right)t - \frac{\pi}{4}\right) \\
-\sqrt{2}J_2\left(\beta_{IF}\right)\cos\left(2\pi\left(f_c - 2f_{IF}\right)t - \frac{\pi}{4}\right) - J_1\left(\beta_{LO}\right)\cos\left(2\pi\left(f_c + f_{LO}\right)t\right) \\
+J_1\left(\beta_{LO}\right)\sqrt{c_1\left(f_c - f_{LO}\right)}\cos\left(2\pi\left(f_c - f_{LO}\right)t\right) - J_2\left(\beta_{LO}\right)\cos\left(2\pi\left(f_c + 2f_{LO}\right)t\right) \\
-J_2\left(\beta_{LO}\right)\sqrt{c_1\left(f_c - 2f_{LO}\right)}\cos\left(2\pi\left(f_c - 2f_{LO}\right)t\right)
\end{bmatrix}
\tag{6}
$$

where $c_1(f_c - f_{LO})$ and $c_1(f_c - 2f_{LO})$ are the amount of suppression in the first and second order lower LO sideband respectively, caused by the optical filter. The output of the optical filter is detected by a photodetector. Beating between various frequency components at the photodetector generate photocurrents at the desired up converted RF signal frequency of $f_{LO} - f_{IF}$, which is referred to as the LSB, the LO frequency of f_{LO}, and the undesired USB frequency of $f_{LO} + f_{IF}$. They can be obtained from (6) and are given by

$$
I_{LO-IF} = \frac{-\Re P_{in}t_{ff}}{8}J_1(\beta_{IF})J_1(\beta_{LO})
\tag{7}
$$

$$
I_{LO} = \frac{\Re P_{in}t_{ff}}{16}J_1(\beta_{LO})\left\{\left[\kappa\cos\theta\left(1 - \sqrt{c_1\left(f_c - f_{LO}\right)}\right) + J_2(\beta_{LO})\left(1 - \sqrt{c_1\left(f_c - f_{LO}\right)c_1\left(f_c - 2f_{LO}\right)}\right)\right]^2\right.
$$

$$
\left. + \left[\kappa\sin\theta\left(1 + \sqrt{c_1\left(f_c - f_{LO}\right)}\right)\right]^2\right\}^{1/2}
\tag{8}
$$

$$
I_{LO+IF} = \frac{-\Re P_{in}t_{ff}}{8}J_1(\beta_{IF})J_1(\beta_{LO})\sqrt{c_1\left(f_c - f_{LO}\right)}
\tag{9}
$$

where $\Re$ is the photodetector responsivity, P_{in} is the CW light power into the DPMZM, $\kappa = (A^2 + B^2)^{1/2}$, $\theta = \tan^{-1}(B/A)$, and

$$
A = -J_0(\beta_{IF}) + \sqrt{1 + J_0^2(\beta_{LO})}\cos\left(\tan^{-1}\frac{1}{J_0(\beta_{LO})}\right)
\tag{10}
$$

$$
B = -J_0(\beta_{IF}) + \sqrt{1 + J_0^2(\beta_{LO})}\sin\left(\tan^{-1}\frac{1}{J_0(\beta_{LO})}\right)
\tag{11}
$$

The photocurrent at the LO frequency given in (8) is caused by beating between the first order LO sidebands with the residual optical carrier and the second order LO sidebands at the photodetector. Since both the first and second order upper LO sidebands are inside the optical filter passband, beating between these sidebands at the photodetector is the major contribution to the LO photocurrent. Beating between the second order upper LO sideband and the first order IF sideband generates a frequency component at $2f_{LO} - f_{IF}$, which is far away from the up converted RF signal at $f_{LO} - f_{IF}$, and hence it can easily be filtered out by a lowpass filter. The LO (sideband) suppression ratio, which is defined as the electrical power ratio of the LO (undesired sideband) to the desired up converted RF signal, can be obtained from (7)–(11). Simulation results show, using an LO modulation index of 0.14 and an optical filter to suppress the first order lower LO sideband by 30 dB, the LO and sideband suppression ratio is 31.8 dB and 30 dB respectively. Note that the second order IF sidebands shown in Fig. 1(b) can also beat with the LO sidebands, which generate undesired frequency components at $f_{LO} \pm 2f_{IF}$ that are close to the up converted RF signal. The photocurrents of these frequency components can be obtained from (6). They have the same
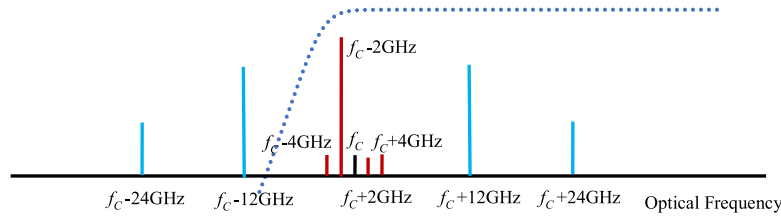
Fig. 2. Optical spectrum at the output of the DPMZM shown in Fig. 1(a) when the DDMZMs are driven by a 2 GHz IF signal and a 12 GHz LO, and the optical filter amplitude response (dotted line).

amplitude and are given by

$$I_{LO\pm2IF} = \frac{\Re P_{in}t_{ff}}{16}\sqrt{2}J_2(\beta_{IF})J_1(\beta_{Lo})\sqrt{c_1(f_c - f_{LO}) + 1} \qquad (12)$$

The second order sideband suppression ratio, which is defined as the electrical power ratio of the frequency components at $f_{LO} \pm 2f_{IF}$ to the desired up converted RF signal, can be obtained from (7) and (12), and is found to be 35 dB. This shows the undesired microwave frequency components at the output of the microwave photonic frequency up converter shown in Fig. 1(a) are more than 30 dB below the desired LSB, i.e., the up converted RF signal. This agrees with the simulation results obtained using a photonic simulation software.

Note that there are two quadrature points with an opposite-slope in an MZM transfer characteristic [15]. In the above analysis, the top DDMZM inside the DPMZM is biased at the negative-slope quadrature point to eliminate the lower IF sideband. Biasing the top DDMZM at the positive-slope quadrature point can eliminate the upper IF sideband. Hence the proposed SSB mixer can generate an up converted RF signal at the frequency of either $f_{LO} - f_{IF}$ or $f_{LO} + f_{IF}$ by simply controlling a modulator bias voltage, rather than using an electrical switch in the SSB mixer presented in [9]. Note that the only electrical component used in the structure shown in Fig. 1(a) is a low-frequency 90° hybrid coupler for generating two quadrature-phase low-frequency IF signals into the top DDMZM. Therefore, the upper operating frequency of the proposed SSB mixer is only limited by the bandwidth of the DPMZM.

Simulation results show a 30-dB suppression in the lower LO sideband, i.e., $c_1(f_c - f_{LO}) = -30$ dB, is required in order to ensure the proposed SSB mixer has more than 30 dB suppression ratio. The amount of the lower LO sideband suppression is determined by the sharpness of the optical filter response edge. For example, the SSB mixer shown in Fig. 1(a) is designed to up convert a 2 GHz IF signal into a 14 GHz RF signal by using a 12 GHz LO. In this case, the optical spectrum at the output of the DPMZM is shown in Fig. 2. An up converted RF signal at 14 GHz is generated by the beating of the lower IF sideband at $f_c - 2$ GHz with the upper LO sideband at $f_c + 12$ GHz at the photodetector. The centre frequency of the optical filter needs to be designed to pass the lower IF sideband and to suppress the lower LO sideband by more than 30 dB. It can be seen from Fig. 2 that the frequency separation between the lower IF and LO sideband is 10 GHz. Hence the optical filter edge roll-off needs to be 3 dB/GHz or 375 dB/nm, which can be achieved by commercial optical filters such as a tunable filter (XTM-50) from EXFO.

3. Experimental Results

An experiment was set up as shown in Fig. 1(a) to verify the concept of the DPMZM based SSB mixer. A tunable laser (Keysight N7711A) was used to generate CW light with 100 kHz linewidth and 12 dBm optical power. The light was launched into a DPMZM (Sumitomo T.SBZH1.5-20PD-ADC-P-LC) via a polarisation controller (PC), which was used to align the light polarisation state into the modulator to maximise the modulation efficiency. Due to the lack of a low-frequency 90° hybrid coupler at the time of experiment, an RF signal generator and a 2–18 GHz bandwidth 90° hybrid coupler were used to generate two quadrature-phase IF signals into a DDMZM inside the DPMZM. The other DDMZM was driven by an LO as shown in Fig. 1(a). Four low-cost optical bandpass filters
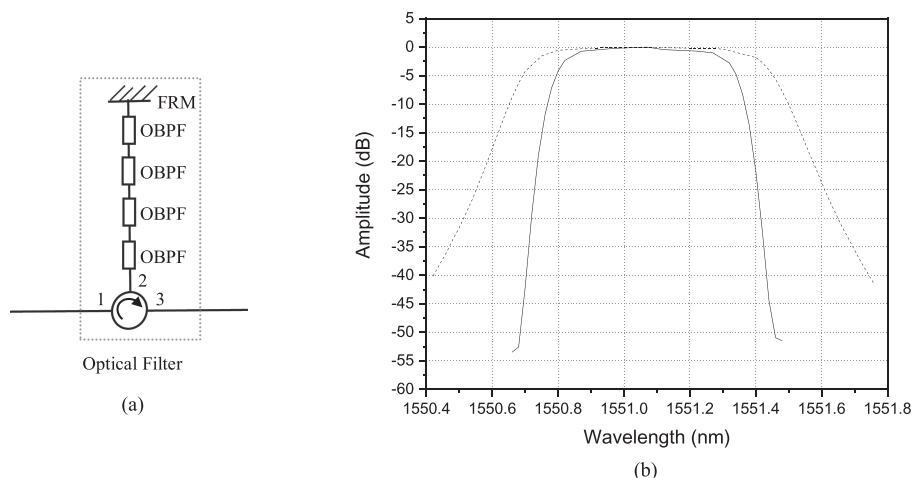
Fig. 3. (a) Setup of the optical filter used in the experiment to suppress the lower LO sideband. (b). Measured normalized amplitude response of a standard DWDM optical bandpass filter (dotted) and the optical filter (solid) implemented by an optical circulator, four DWDM optical bandpass filters and an FRM.

(OBPFs) and a Faraday rotator mirror (FRM) were connected to Port 2 of an optical circulator as shown in Fig. 3(a) to implement a sharp edge roll-off optical filter. All four OBPFs were standard DWDM bandpass filters having 1550.92 nm centre wavelength and 0.6 nm 3-dB bandwidth. Fig. 3(b) shows the amplitude responses of one of the OBPFs and the overall optical filter. It shows the roll-off of the overall optical filter amplitude response edge is 403 dB/nm. According to the theoretical analysis, this enables the SSB mixer to obtain >30 dB suppression ratio when it operates at the frequencies of >12 GHz. The insertion loss of the overall optical filter was 7.1 dB. An erbium-doped fibre amplifier (EDFA) was connected to Port 3 of the optical circulator to compensate for the system loss. This was followed by a tunable optical filter with 0.5 nm 3-dB bandwidth for suppressing the amplified spontaneous emission noise generated by the EDFA. The optical signal at the output of the SSB mixer was detected by a photodetector (Discovery Semiconductor DSC30S).

A 2 GHz IF signal and a 16 GHz LO were applied separately to the two quadrature-biased DDMZMs inside the DPMZM. The tunable laser wavelength was set to 1550.82 nm to obtain a large suppression in the lower LO sideband. The LO power and the bias voltage of the main MZM in the DPMZM were adjusted to suppress the optical carrier at the output of the DPMZM. The SSB mixer output optical spectrum in Fig. 4(a) shows the upper IF and LO sidebands together with the upper second order LO sideband. It can be seen from the figure that there is over 33 dB suppression in the lower LO sideband. By biasing the DDMZM driven by the IF signal at another quadrature point in the modulator transfer characteristic, a lower IF sideband rather than an upper IF sideband was obtained and is shown in Fig. 4(b). The corresponding SSB mixer output electrical spectrums were measured using an electrical signal analyser connected to the photodetector output. The EDFA gain was adjusted so that the average output optical power was 5 dBm. Fig. 5 shows an up converted RF signal at 14 GHz and 18 GHz, which correspond to the LSB and the USB respectively, when the DDMZM driven by an IF signal inside the DPMZM was biased at the negative-slope and positive-slope quadrature point. The results demonstrate the LO, undesired sideband and harmonic components are largely suppressed for the mixer operated in either a LSB or USB mode, and the two modes can be switched by simply adjusting a modulator bias voltage.

The performance of the SSB mixer for different input LO frequencies was investigated. The IF signal frequency was fixed at 2 GHz and the DDMZM driven by an IF signal was biased at the negative-slope quadrature point so that the SSB mixer was operated in the LSB mode. Fig. 6(a) shows the power of the desired LSB has only 2 dB change as the LO frequency changes from 12 GHz to 20 GHz. The power of the LO, the undesired USB and the second order sideband at $f_{LO} - 2f_{IF}$ relative to the LSB power were also measured and are shown in the figure. Around
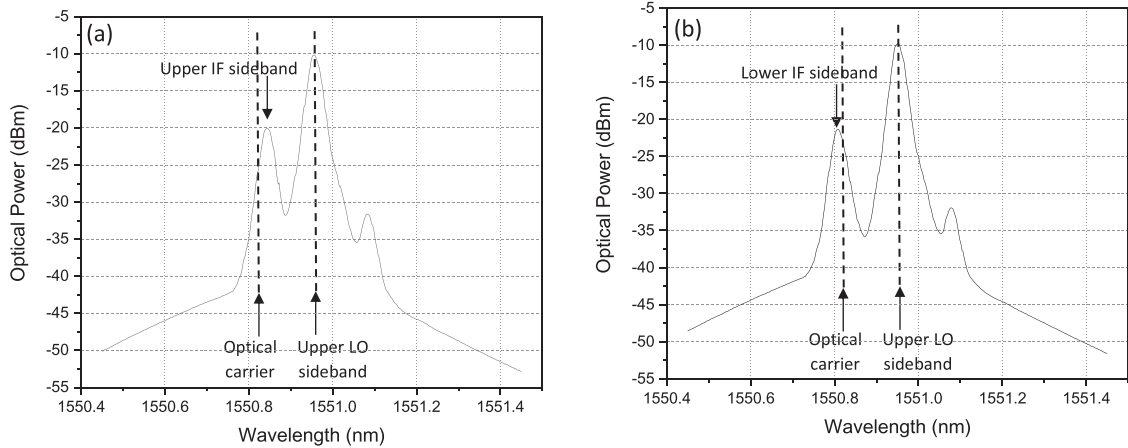
Fig. 4. Measured SSB mixer output optical spectrum when the DDMZM driven by an IF signal inside the DPMZM was biased at the (a) negative-slope and (b) positive-slope quadrature point.
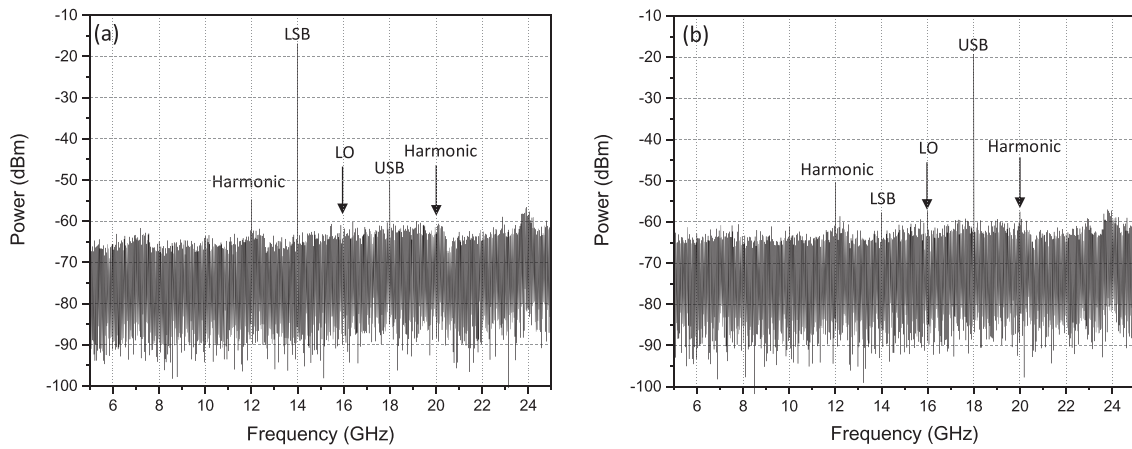

Fig. 5. Measured output electrical spectrum of the SSB mixer when it operated in the (a) LSB and (b) USB mode.
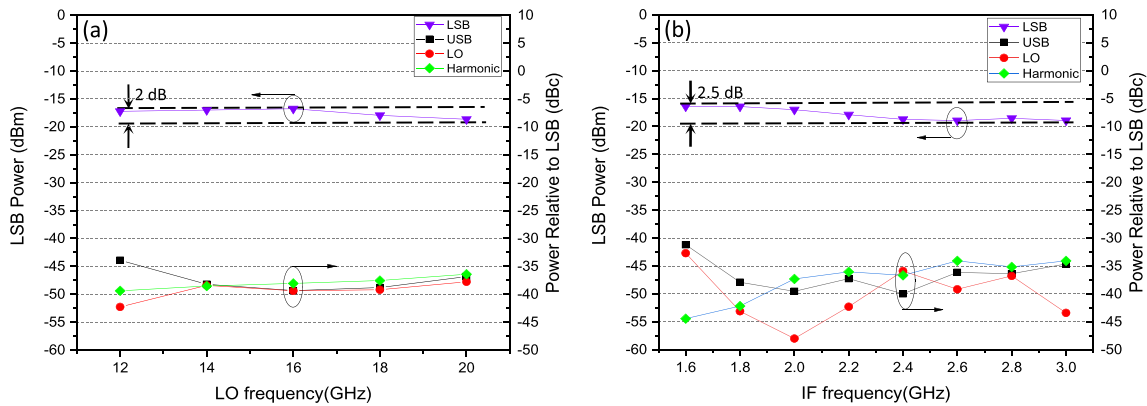

Fig. 6. Measured desired LSB power, and the LO power, the USB power and the second order sideband power relative to the LSB power versus (a) the LO frequency and (b) the IF signal frequency when the DPMZM based SSB mixer is operated in the LSB mode.
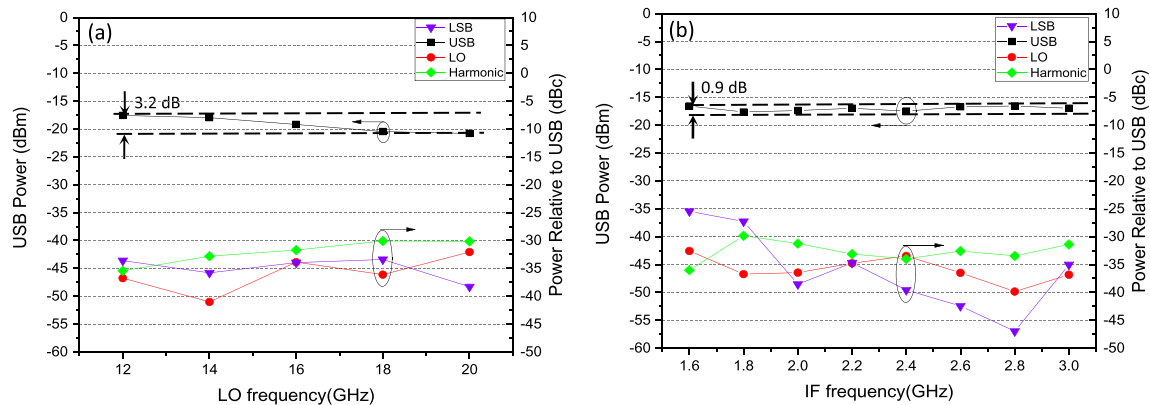
Fig. 7. Measured desired USB power, and the LO power, the LSB power and the second order sideband power relative to the USB power versus (a) the LO frequency and (b) the IF signal frequency when the DPMZM based SSB mixer is operated in the USB mode.

35 dB suppression ratio in the LO, undesired USB and second order sideband was obtained. The undesired USB to the desired LSB suppression ratio reduced at 12 GHz LO frequency. This is because the amount of the lower LO sideband suppression reduces as the LO sideband moves closer to the optical carrier. In order to demonstrate the SSB mixer can operate at different IF signal frequencies, the LO frequency was fixed at 18 GHz and the IF signal frequency was changed from 1.6 to 3 GHz with a 0.2 GHz step. As shown in Fig. 6(b), the power of the LSB has less than 3 dB fluctuation and is more than 31 dB higher than the LO, undesired USB and second order sideband throughout the 1.6 to 3 GHz IF frequency range. Note that the undesired USB suppression ratio reduces as the input IF signal frequency reduces to below 2 GHz. This is due to the phase imbalance of the 2–18 GHz bandwidth 90° hybrid coupler increases when the input IF signal frequency is outside the hybrid coupler bandwidth. The above measurements were repeated after biasing the DDMZM driven by an IF signal at the positive-slope quadrature point so that the SSB mixer was operated in the USB mode. Fig. 7(a) shows the desired USB has around 3 dB power fluctuation and the SSB mixer has over 30 dB suppression ratio for 12 to 20 GHz input LO frequency. Fig. 7(b) shows little changes in the desired USB power and over 30 dB suppression ratio for an input IF signal frequency of 2 to 3 GHz. The experimental results shown in Fig. 6 and 7 demonstrate SSB mixing up to 20 GHz. This was limited by the upper operating frequency of the RF signal generator used in the experiment. In order for the SSB mixer to operate in the 60 GHz band, an RF signal generator that is capable to generate a high-frequency millimetre wave LO is needed. A DPMZM and a photodetector with a 60 GHz bandwidth are also required. Since, in this case, the LO sidebands are ±60 GHz away from the optical carrier, the edge roll-off requirement of the optical filter is relaxed compared to that when up converting an IF signal into the 12–20 GHz band in the experimental demonstration. Hence a single standard DWDM optical bandpass filter with an amplitude response as shown by the dotted line in Fig. 3(b) can be employed to obtain more than 30 dB suppression in the lower LO sideband while passing the IF and upper LO sidebands.

4. Conclusion

A new microwave photonic SSB mixer has been presented. It is based on a DPMZM formed by two quadrature-biased DDMZMs connected in parallel, which generate an SSB IF modulated optical signal and a DSB LO modulated optical signal. The optical carrier is cancelled at the output of the DPMZM by designing the LO modulation index and biasing the main MZM in the DPMZM at the null point. This consequently suppresses the output LO. The undesired sideband at the mixer output is suppressed by using an optical filter to remove the lower LO sideband. The SSB mixer has a simple structure and does not require broadband electrical components. It can be switched

between the LSB and the USB mode by adjusting a modulator bias voltage. The LO modulation index and the optical filter amplitude response edge roll-off required for the SSB mixer to obtain an over 30 dB suppression ratio have been analysed. Experimental results demonstrate around 30 dB suppression in the LO, undesired sideband and second order sideband for different input LO and IF signal frequencies.

References

[1] X. Fernando, "Radio over fiber-an optical technique for wireless access," in *Proc. IEEE Sarnoff Symp.*, 2009.

[2] J. Park, M. S. Shakouri, and K. Y. Lau, "Millimetre-wave electro-optical upconverter for wireless digital communications," *Electron. Lett.*, vol. 31, no. 13, pp. 1085–1086, 1995.

[3] Y. L. Guennec, G. Maury, J. Yao, and B. Cabon, "New optical microwave up-conversion solution in radio-over-fiber networks for 60-GHz wireless applications," *J. Lightw. Technol.*, vol. 24, no. 3, pp. 1277–1282, Mar. 2006.

[4] C. S. Park, C. K. Oh, C. G. Lee, D. H. Kim, and C. S. Park, "A photonic up-converter for a WDM radio-over-fiber system using cross-absorption modulation in an EAM," *IEEE Photon. Technol. Lett.*, vol. 17, no. 9, pp. 1950–1952, Sep. 2005.

[5] J. S. Lee, H. J. Song, W. B. Kim, M. Fujise, Y. H. Kim, and J. I. Song, "All-optical harmonic frequency upconversion of radio over fibre signal using cross-phase modulation in semiconductor optical amplifier," *Electron. Lett.*, vol. 40, no. 19, pp. 1211–1213, 2004.

[6] C. S. Park, C. G. Lee, and C. S. Park, "Photonic frequency upconversion based on stimulated Brillouin scattering," *IEEE Photon. Technol. Lett.*, vol. 19, no. 10, pp. 777–779, May 2007.

[7] J. H. Seo, C. S. Choi, Y. S. Kang, Y. D. Chung, J. Kim, and W. Y. Choi, "SOA-EAM frequency up/down-converters for 60-GHz bi-directional radio-on-fiber systems," *IEEE Trans. Microw. Theory Tech.*, vol. 54, no. 2, pp. 959–966, Feb. 2006.

[8] Z. Xu, X. Zhang, and J. Yu, "Frequency upconversion of multiple RF signals using optical carrier suppression for radio over fiber downlinks," *Opt. Exp.*, vol. 15, no. 10, pp. 16737–16747, 2007.

[9] Z. Tang and S. Pan, "A filter-free photonic microwave single sideband mixer," *IEEE Microw. Wireless Compon. Lett.*, vol. 26, no. 1, pp. 67–69, Jan. 2016.

[10] Y. Wang *et al.*, "Microwave photonic mixer with large mixing spurs suppression and high RF/LO isolation," *Optik*, vol. 174, pp. 630–635, 2018.

[11] Z. Tang and S. Pan, "A compact image-reject and single-sideband mixer with suppression of LO leakage based on a dual-polarization dual-drive Mach-Zehnder modulator," in *Proc. IEEE Int. Top. Meeting Microw. Photon.*, 2016, pp. 79–82.

[12] Y. Gao, A. Wen, W. Jiang, Y. Fan, Y. He, and D. Zhou, "Fundamental/subharmonic photonic microwave I/Q up-converter for single sideband and vector signal generation," *IEEE Trans. Microw. Theory Tech.*, vol. 66, no. 9, pp. 4282–4292, Sep. 2018.

[13] Y. Gao, A. Wen, W. Jiang, Y. Fan, D. Zhou, and Y. He, "Wideband photonic microwave SSB up-converter and I/Q modulator," *J. Lightw. Technol.*, vol. 35, no. 18, pp. 4023–4032, Sep. 2017.

[14] J. D. Downie and A. B. Ruffin, "Analysis of signal distortion and crosstalk penalties induced by optical filters in optical networks," *J. Lightw. Technol.*, vol. 21, no. 9, pp. 1876–1886, Sep. 2003.

[15] B. Vidal, J. L. Corral, and J. Marti, "All-optical WDM microwave filter with negative coefficients," *IEEE Photon. Technol. Lett.*, vol. 17, no. 3, pp. 666–668, Mar. 2005.